

Bridging Semantics and Geometry: A Decoupled LVLM–SAM Framework for Reasoning Segmentation in Remote Sensing

Xu Zhang, Junyao Ge, Yang Zheng, Kaitai Guo, Jimin Liang*

School of Electronic Engineering, Xidian University, Xi'an, Shaanxi 710071, China

Abstract

Large Vision–Language Models (LVLMs) hold great promise for advancing remote sensing (RS) analysis, yet existing reasoning segmentation frameworks couple linguistic reasoning and pixel prediction through end-to-end supervised fine-tuning, leading to weak geometric grounding and limited generalization across tasks. To address this, we developed Think2Seg-RS, a decoupled framework that trains an LVLM prompter to control a frozen Segment Anything Model (SAM) via structured geometric prompts. Through a mask-only reinforcement learning objective, the LVLM learns to translate abstract semantic reasoning into spatially grounded actions, achieving state-of-the-art performance on the EarthReason dataset. Remarkably, the learned prompting policy generalizes zero-shot to multiple referring segmentation benchmarks, exposing a distinct divide between semantic-level and instance-level grounding. We further found that compact segmenters outperform larger ones under semantic-level supervision, and that negative prompts are ineffective in heterogeneous aerial backgrounds. Together, these findings establish semantic-level reasoning segmentation as a new paradigm for geospatial understanding, opening the way toward unified, interpretable LVLM-driven Earth observation. Our code and model are available at <https://github.com/Ricardo-XZ/Think2Seg-RS>.

Keywords: Remote sensing, reasoning segmentation, Large Vision Language Model, Segment Anything Model, reinforcement learning

1. Introduction

Segmentation of remote sensing (RS) imagery has long been recognized as a cornerstone of intelligent image interpretation. Over the years, segmentation techniques have evolved from *semantic segmentation*, which assigns a fixed class label to every pixel (Yuan et al., 2021; Lv et al., 2023; Guo et al., 2019; Ma et al., 2024), to *instance segmentation*, which further distinguishes individual objects of the same category (Chen et al., 2024a; Xu et al., 2021; Liu et al., 2024b; Su et al., 2020), with illustrative examples provided in Fig. 1. While these approaches have achieved notable progress, existing paradigms remain inherently constrained by predefined label sets and therefore struggle to cope with open-world conditions where user needs cannot be fully anticipated.

To overcome this rigidity, *referring expression segmentation* is proposed (Yuan et al., 2024; Liu et al., 2024a; Lei et al., 2025; Pan et al., 2024; Yao et al., 2025a; Dong et al., 2024), enabling users to specify targets through natural language descriptions of their visual attributes, such as category names, colors, or spatial positions (e.g., “the red small vehicle on the top left,” see Fig. 1). However, real-world queries are often implicit and compositional, going beyond observable attributes to involve conditions like spatial context, causal relations, or geographic commonsense, for instance, “Identify the sports area

that is most suitable for hosting a hurdle competition.” Addressing such queries requires models that can simultaneously (i) interpret implicit natural language instructions, (ii) reason about spatial relations, causal logic, and domain knowledge, and (iii) deliver precise pixel-level delineations. This emerging paradigm, termed *reasoning segmentation* (Li et al., 2025; Yao et al., 2025b), represents the latest stage in the progression of RS segmentation methods.

Although Large Vision–Language Models (LVLMs) have demonstrated impressive instruction following and multimodal reasoning on natural images, directly applying them to RS is far from sufficient. In terms of training data and objectives, mainstream LVLMs (e.g., LLaVA-1.5 (Liu et al., 2023), InternVL3 (Zhu et al., 2025), and Qwen-2.5-VL (Bai et al., 2025), which are the open-source models we adopt in our study) are primarily optimized for image–text instruction following, visual question answering, document understanding, and grounding with boxes, rather than dense, pixel-accurate segmentation masks. This mismatch yields domain gaps (e.g., nadir views, tiny objects, repetitive textures, and geographic semantics that differ markedly from the natural images dominating current LVLM training corpora) and task gaps (e.g., from captioning/question-answering or box-level grounding to fine-grained mask delineation). Even if an LVLM correctly parses an implicit query, converting its reasoning into reliable, fine-grained masks remains nontrivial because current LVLM heads and training signals are not tailored for precise spatial delineation. Moreover, early RS reasoning-segmentation pipelines that map compressed LVLM

*Corresponding author.

Email address: jimleung@mail.xidian.edu.cn (Jimin Liang)

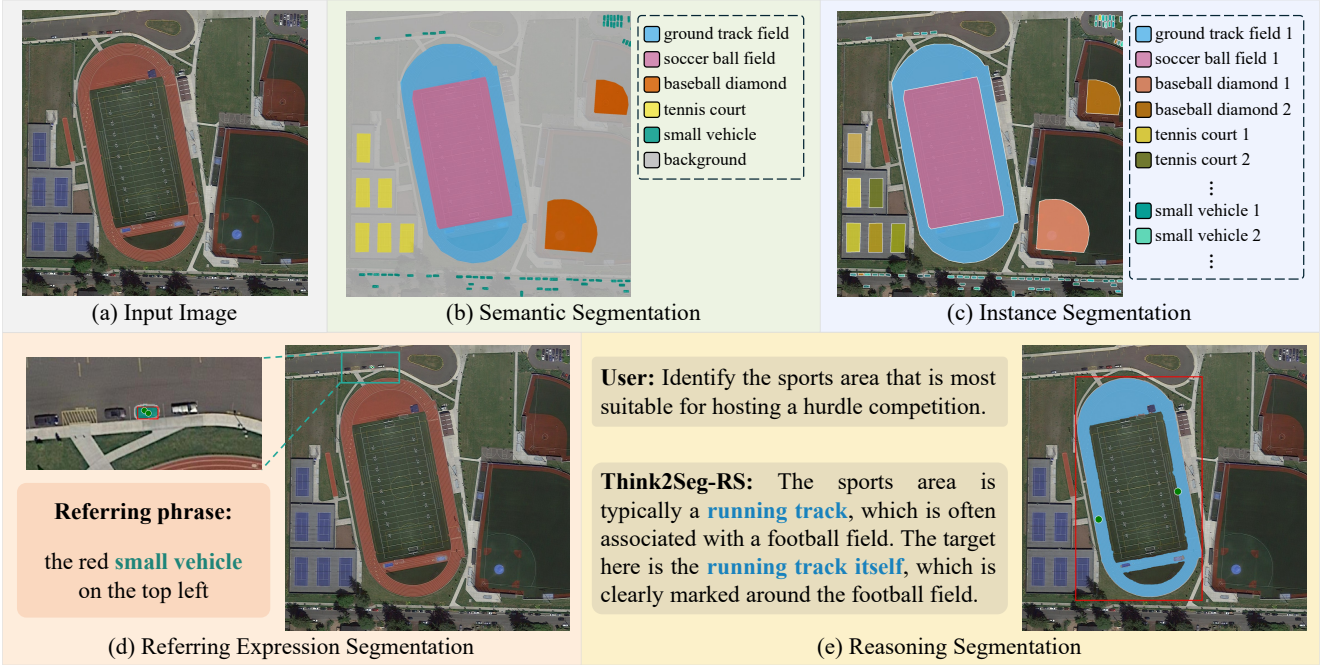


Fig. 1: Illustration of the evolution of segmentation paradigms in RS imagery. (a) Input image sampled from the iSAID dataset (Waqas Zamir et al., 2019). (b) Semantic segmentation ground truth provided by the dataset, assigning fixed class labels to every pixel. (c) Instance segmentation ground truth, distinguishing individual objects of the same class. (d) Referring expression segmentation result (mask and generated prompts, box in red and positive points in green) produced by our proposed Think2Seg-RS method, guided by explicit language queries. (e) Reasoning segmentation result by Think2Seg-RS, handling implicit, compositional queries.

embeddings directly to masks with a monolithic decoder suffer from information bottlenecks, limited interpretability, and restricted architectural scalability (Li et al., 2025).

To address these challenges, we propose a decoupled reasoning–execution framework that explicitly separates reasoning from segmentation. In this design, an LVLM serves as the reasoning module, interpreting complex or implicit instructions and emitting structured geometric prompts (bounding boxes and points), while a universal segmenter acts as the execution module to translate prompts into masks. The Segment Anything Models (SAMs) (Kirillov et al., 2023; Ravi et al., 2024) are particularly suited for this role due to their strong zero-shot generalization and promptable interfaces; their RS variants already show robust performance (Ren et al., 2024a; Wang et al., 2023; Zheng et al., 2024).

The practical bottleneck in RS therefore lies not in the segmentation capacity of SAM itself, but in how to generate suitable prompts that bridge high-level reasoning with low-level execution. Concretely, this involves (i) *semantic grounding*—mapping implicit, compositional queries to the correct subset of instances and their spatial extents; (ii) *spatial precision and instance control*—deciding where and how prompts (e.g., boxes and points) should be issued so that SAM yields accurate masks under scale variation, clutter, and ambiguous boundaries; and (iii) *automation at scale*—eliminating the brittleness and cost of manual prompt design. Our solution is to train the LVLM to automatically generate such high-quality prompts that faithfully reflect both user intent and RS scene context, while keeping SAM frozen to preserve its universality and avoid domain-specific

retraining.

Building on this idea, we present Think2Seg-RS, a training-efficient framework for RS reasoning segmentation. In our design, the LVLM (Qwen-2.5-VL family) is the only trainable component and is optimized to produce well-formed JSON-structured prompts (a bounding box plus two positive points per instance) from image–text inputs, while a frozen SAM2 (Ravi et al., 2024) executes segmentation conditioned on these prompts. To bridge the reasoning–segmentation gap, we adopt Group Relative Policy Optimization (GRPO) (Shao et al., 2024) with a simple, result-oriented reward composed of (i) an output-format reward (ensuring valid `<think>/<answer>` tags and JSON) and (ii) the final Intersection-over-Union (IoU) of the SAM-produced mask. This establishes a direct feedback loop from segmentation outcomes to prompt generation, enabling the LVLM to learn a reasoning-to-segmentation skill that generalizes beyond hand-crafted prompting strategies and yields a mask-only, modular training recipe.

Recent concurrent works such as Seg-Zero (Liu et al., 2025a), VisionReasoner (Liu et al., 2025b), and RemoteReasoner (Yao et al., 2025b) also adopt decoupled LVLM–SAM paradigms with reinforcement learning to generate prompts for segmentation. However, these approaches depend on pseudo box–point supervision, which constrains flexibility and adds annotation overhead. In contrast, Think2Seg-RS demonstrates that a mask-only optimization scheme is sufficient to equip LVLMs with effective prompting skills for RS reasoning segmentation, enlarging the search space for prompting strategies, reducing annotation cost, and offering a more scalable and efficient alternative.

In summary, our contributions are threefold:

- **Decoupled reasoning–execution.** We formalize RS reasoning segmentation within a decoupled reasoning–execution framework and introduce Think2Seg-RS, which separates high-level language understanding and reasoning (LVLM) from low-level pixel execution (SAM). This design eliminates manual prompt engineering and domain-specific fine-tuning, while preserving modularity and plug-and-play adaptability to future LVLMs.
- **Mask-only GRPO optimization.** We develop a lightweight optimization scheme based on GRPO that uses only mask annotations and a simple IoU + format reward, avoiding costly instance-level box–point supervision and equipping the LVLM with a robust reasoning-to-prompt capability.
- **SOTA accuracy and transfer.** Think2Seg-RS sets new state-of-the-art (SOTA) results on the EarthReason reasoning segmentation dataset (Li et al., 2025) and exhibits strong zero-shot transfer to the RRSIS-D (Liu et al., 2024a), RISBench (Dong et al., 2024) and RefSegRS (Yuan et al., 2024) referring expression segmentation benchmarks, evidencing that the learned prompting policy generalizes across datasets and task formulations rather than overfitting to dataset-specific query patterns.

2. Related Work

2.1. From Semantic Labels to Reasoning Segmentation in RS

The evolution of RS image segmentation has followed a clear trajectory. Early work was dominated by semantic (Lv et al., 2023; Yuan et al., 2021; Guo et al., 2019; Ma et al., 2024) and instance segmentation (Chen et al., 2024a; Xu et al., 2021; Liu et al., 2024b; Su et al., 2020), supported by the release of large-scale RS benchmarks (Waqas Zamir et al., 2019; Wang et al., 2021, 2023; Azimi et al., 2019). These methods established strong baselines but remain inherently tied to predefined label sets, limiting their adaptability to open-world scenarios. This challenge has spurred a shift toward more flexible, language-guided paradigms for interactive querying.

Referring expression segmentation represents one such direction, enabling users to locate targets through simple free-form text descriptions. Yuan et al. (2024) first introduced this paradigm into remote sensing, formally defining the task as referring remote sensing image segmentation (RRSIS) and constructing the RefSegRS benchmark dataset to support it. Building on this foundation, Liu et al. (2024a) proposed the RRSIS-D dataset and a Rotated Multi-Scale Interaction Network (RMSIN), which integrates multi-scale interaction and adaptive rotated convolution to better capture the large spatial variations and diverse orientations of objects in aerial scenes. More recently, Pan et al. (2024) identified limitations of the dominant implicit optimization paradigm in RRSIS, namely inter-domain misalignment and semantics-agnostic prediction, and addressed them with a Dual Alignment Network (DANet) that combines explicit affinity alignment and a reliable agent alignment module to enhance cross-modal consistency.

Despite these advances, existing referring expression segmentation methods are fundamentally tailored to explicit expressions, and their alignment strategies remain insufficient for handling implicit, compositional queries that demand deeper reasoning about spatial relationships, causal logic, and geographic commonsense. This gap has motivated the emerging direction of reasoning segmentation. Early explorations have appeared in both the natural image and remote sensing communities. Lai et al. (2024) introduced the concept of *reasoning segmentation* for natural images, proposing the large Language Instructed Segmentation Assistant (LISA) framework to infer segmentation masks from implicit, compositional language queries. Building on this idea, Li et al. (2025) extended the paradigm to the geospatial domain with SegEarth-R1, which pioneered the task of *geospatial pixel reasoning* and released the EarthReason benchmark as the first dedicated dataset for this problem. In this paper, we use the terms *reasoning segmentation* and *geospatial pixel reasoning* interchangeably, as they denote the same underlying challenge of linking high-level reasoning with fine-grained pixel delineation in RS imagery.

2.2. Universal Execution Engines: SAM for Remote Sensing

As segmentation evolves toward handling implicit, compositional queries, a practical requirement is the ability to generalize beyond fixed taxonomies. The Segment Anything Model (SAM) (Kirillov et al., 2023) aligns well with this need: as a promptable, category-agnostic segmenter, it accepts simple geometric cues (points, boxes, or masks) and exhibits strong zero-shot generalization, thereby reshaping interactive segmentation workflows.

These capabilities have been rapidly explored in the RS domain. Wang et al. (2023) introduced SAMRS, a large-scale RS segmentation corpus constructed by leveraging SAM on existing detection datasets, showing how SAM can bootstrap pixel-level labels at scale. Independent evaluations reported that SAM maintains competitive zero-shot behavior across multiple overhead-imagery benchmarks, further indicating its cross-domain robustness in RS scenes (Ren et al., 2024a). Beyond static single-image settings, Zheng et al. (2024) adapted SAM for bitemporal inputs and formulated Segment Any Change, demonstrating training-free zero-shot change detection via latent-space matching and point queries. Collectively, these studies highlighted SAM’s effectiveness and portability for RS tasks, from single-image segmentation to change detection.

However, SAM’s performance hinges on the quality of its input prompts, creating a bottleneck for large-scale or automated RS pipelines. Recent work therefore focuses on automated prompting. Chen et al. (2024a) proposed RSPrompter, which generates prompt embeddings so that SAM can produce semantically discriminative instance masks in RS imagery. In parallel, Zhang et al. (2023) presented Text2Seg, coupling Grounding DINO for text-to-box grounding with CLIP-derived point cues to steer SAM via language queries. Osco et al. (2023) systematically evaluated SAM for RS applications and discussed practical recipes (e.g., one-shot/lightweight tuning) that can further enhance performance in specific scenarios. These automated strategies are effective when the target is *explicitly* specified (by instance identity or direct text grounding). Yet they are

not designed to infer targets from *implicit* instructions that require multi-step reasoning over spatial relations and geographic commonsense, precisely where a dedicated reasoning module becomes necessary.

2.3. Toward Reasoning-Driven Segmentation with LVLMs

LVLMs have opened a path to language-guided visual reasoning for segmentation. LISA (Lai et al., 2024) establishes the embedding-as-mask paradigm by introducing a <SEG> token that allows an LVLM to interface with a mask decoder, sparking a line of work that explores how LVLMs can guide dense prediction (Yang et al., 2023; Wang and Ke, 2024; Ren et al., 2024b; Bai et al., 2024; Xia et al., 2024; Lan et al., 2025; Chen et al., 2024b). Along this line, LISA++ (Yang et al., 2023) extends from semantic to instance-level segmentation and enables more flexible text interaction, while GSVA (Xia et al., 2024) augments the interface with a <REJ> token to handle empty-target cases. Departing from embedding-as-mask, Text4Seg (Lan et al., 2025) reframes segmentation as text generation: the LVLM outputs coarse masks that are subsequently refined by SAM, avoiding additional decoder training. In contrast, SAM4MLLM (Chen et al., 2024b) fine-tunes the LVLM to directly produce geometric prompts for SAM, sidestepping specialized tokens and architectural changes.

Despite their architectural diversity, these methods all rely on supervised fine-tuning (SFT), treating segmentation as imitation learning with a fixed target per sample. This restricts exploration of alternative prompting strategies and couples performance to large, carefully curated instruction–mask pairs. To move beyond SFT, Seg-Zero (Liu et al., 2025a) and its successor VisionReasoner (Liu et al., 2025b) employs GRPO (Shao et al., 2024) to train an LVLM to generate prompts for SAM2. However, their reward design depends on predefined box–point as intermediate pseudo ground truth, which implies costly instance-level annotations and narrows the search space—limitations that are particularly acute in remote sensing.

The LVLM-driven paradigms have begun to appear in the RS literature as well. For example, GeoPix (Ou et al., 2025) adopts a <SEG>-style interface, while RSUniVLM (Liu and Lian, 2024) and GeoGround (Zhou et al., 2024) follow a Text4Seg-like pipeline to produce masks from language. Yet, these methods focus on *explicit* expressions and struggle with *implicit, compositional* instructions that require multi-step geospatial reasoning. SegEarth-R1 (Li et al., 2025) addresses this gap by formalizing *geospatial pixel reasoning* (i.e., reasoning segmentation in RS) and releasing the EarthReason dataset. However, its architecture couples LVLM embeddings with a specialized mask generator, which reduces modularity, increases training overhead, and compresses reasoning into a single latent embedding, creating an information bottleneck that limits interpretability. RemoteReasoner (Yao et al., 2025b) further adopts a Seg-Zero–style GRPO framework for EarthReason, but still relies on mask-to-box conversion to provide pseudo box–point supervision, inheriting similar annotation and search-space constraints.

Positioning of our approach. Concurrent with recent explorations such as Seg-Zero (Liu et al., 2025a), VisionReasoner (Liu et al., 2025b), and RemoteReasoner (Yao et al., 2025b), which

also adopt a decoupled LVLM–SAM paradigm, we develop Think2Seg-RS for RS reasoning segmentation. The crucial distinction lies in supervision: Seg-Zero and VisionReasoner rely on pseudo box–point labels generated from natural-image datasets, while RemoteReasoner applies mask-to-box conversion on EarthReason—all of them incur costly instance-level prompt supervision and constrain the search space. By contrast, Think2Seg-RS is optimized with GRPO using only mask annotations and a simple result-oriented reward (IoU + format). This mask-only optimization enlarges the exploration space for prompting, reduces annotation cost, and improves scalability to RS reasoning segmentation tasks.

3. METHODOLOGY

3.1. Think2Seg-RS Framework

The architecture of Think2Seg-RS, illustrated in Fig. 2, follows a two-stage decoupled reasoning–execution design that combines a trainable LVLM prompter with a frozen segmentation engine. Specifically, we adopt Qwen-2.5-VL (Bai et al., 2025) as the LVLM prompter and SAM2 (Ravi et al., 2024) as the universal segmenter. This division of labor delegates high-level reasoning and language understanding to the prompter, while the segmenter is responsible for robust pixel-level execution. Given a remote sensing image $I \in \mathbb{R}^{H \times W \times 3}$ and a complex natural language query Q , the framework proceeds in two stages.

3.1.1. Reasoning and Prompting

The LVLM prompter is the only trainable component of the framework and serves as the reasoning module. Upon receiving the input pair (I, Q) , together with an instruction template that guides its reasoning process (see Fig. Appendix A.1), the prompter performs two tasks.

First, it generates a Chain-of-Thought (CoT) enclosed in <think> and </think> tags, verbalizing its interpretation of the query in the context of the RS scene (e.g., “The facility being referred to is likely an oil or chemical storage tank, which is typically monitored for leaks...”). This step enhances reasoning robustness and provides interpretability.

Second, conditioned on this reasoning, the prompter produces structured geometric prompts for SAM2, denoted as P in JSON format within <answer> tags. Each such prompt specifies one bounding box and two positive points for a target instance, while an empty list $[]$ is returned when no target is present to preserve JSON validity. For subsequent formulation, we denote this prompt set abstractly as P , from which coordinate sets are derived and passed to the segmenter for execution.

3.1.2. Segmentation Execution

The prompts P are parsed into coordinate sets P_{geom} , each corresponding to a target instance. For instance i , the SAM2 segmenter takes $(I, P_{\text{geom}}^{(i)})$ as input and produces a binary mask $M^{(i)} \in \{0, 1\}^{H \times W}$. When multiple instances are present, the final mask is aggregated by logical union $M = \bigcup_{i=1}^N M^{(i)}$, where N denotes the number of detected instances. This instance-aware execution ensures accurate delineation of each object while preserving spatial coherence across the entire scene.

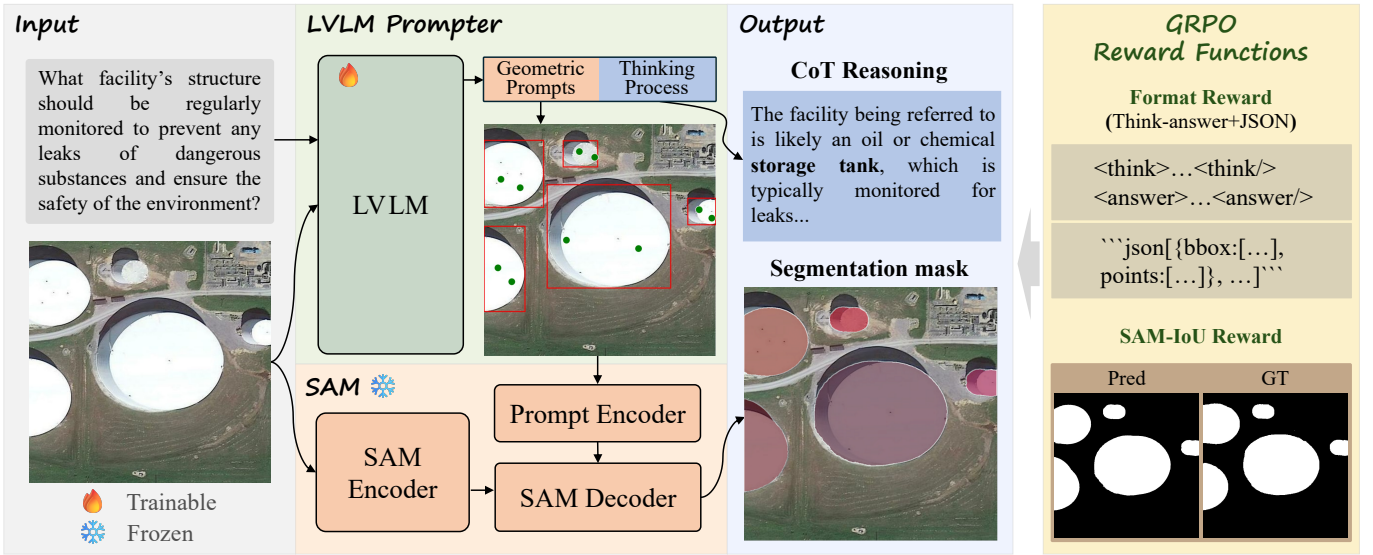


Fig. 2: Architecture of Think2Seg-RS. A trainable LVLM prompter interprets the image–query pair, generates CoT reasoning, and outputs structured JSON prompts optimized via GRPO. These prompts are then executed by a frozen segmenter (SAM) to produce the final segmentation masks.

3.1.3. Framework Characteristics

This decoupled reasoning–execution architecture separates high-level reasoning from low-level segmentation: the LVLM prompter serves as the reasoning module, while the frozen segmenter ensures reliable execution. Within this design, the task can be further reframed as a more tractable reasoning-to-prompt problem, where the prompter learns to infer and generate high-quality geometric prompts that faithfully reflect user intent, and the segmenter converts these prompts into precise masks. In doing so, Think2Seg-RS avoids costly fine-tuning of SAM, enhances modularity, and ensures scalability to future LVLMs, while the explicit CoT process equips the system to handle complex, implicit queries that are characteristic of RS imagery.

3.2. Mask-Only GRPO Optimization for Prompt Learning

A central challenge in our framework lies in training the LVLM to generate effective prompts that faithfully bridge high-level reasoning with low-level segmentation. A naive zero-shot application of general-purpose LVLMs such as Qwen-2.5-VL (Bai et al., 2025) or InternVL3 (Zhu et al., 2025) to RS imagery often produces inaccurate localization, with misaligned bounding boxes or poorly placed points, highlighting the need for robust task-specific adaptation.

A conventional supervised fine-tuning strategy, however, is ill-suited for this problem. For any given image I and query Q , there exists a virtually infinite space of prompt *combinations* (the number and types of prompts, e.g., boxes or points) and *geometries* (the precise size and coordinates) that could yield correct segmentation. Consequently, there is no unique ground-truth prompt to serve as a fixed supervision target. Forcing the model to mimic a single pseudo prompt, as done in Seg-Zero (Liu et al., 2025a), VisionReasoner (Liu et al., 2025b), and RemoteReasoner (Yao et al., 2025b), introduces behavioral cloning bias, restricts exploration to handcrafted or converted box–point an-

notations, and incurs annotation overhead that limits scalability in RS settings.

To overcome these limitations, we propose a mask-only reinforcement learning paradigm built on three design choices. First, we employ the GRPO algorithm (Shao et al., 2024), which efficiently leverages relative rewards among multiple candidates per query to stabilize large-model training. Second, we adopt a simple, result-oriented reward that directly evaluates the SAM2-produced mask: it consists of (i) a format reward ensuring valid $\langle\text{think}\rangle/\langle\text{answer}\rangle$ tags and JSON outputs, and (ii) an IoU reward measuring overlap with the ground-truth mask. This direct feedback loop aligns prompt generation with final segmentation quality, avoiding the need for costly pseudo box–point supervision. Third, we fix the prompt combination to a universally effective set for RS targets (one bounding box and two positive points per instance), reducing the action space and making exploration tractable, while leaving the LVLM free to optimize spatial placement.

This mask-only GRPO optimization enables the LVLM to autonomously discover prompting strategies that generalize beyond handcrafted heuristics, enlarging the search space, reducing annotation cost, and enhancing scalability for RS reasoning segmentation.

3.2.1. GRPO-based Prompt Optimization

In our framework, the LVLM itself serves as the policy model π_θ , responsible for generating structured JSON prompts given an image I and query Q . To enable exploration, for each (I, Q) pair we draw a set of G candidate prompt outputs $O = \{o_1, o_2, \dots, o_G\}$, sampled from the old policy $\pi_{\theta_{\text{old}}}$ via stochastic decoding. Here, diverse candidates are drawn from the model’s output distribution for relative comparison. For each candidate $o_i \in O$, the frozen SAM2 performs segmentation conditioned on o_i , producing a mask from which a task-specific reward $r_i = R(o_i)$ is computed (detailed in Eq. 3).

GRPO optimizes the LVLM by comparing the relative quality of candidates within each sampled group. Specifically, the rewards $\{r_1, \dots, r_G\}$ are normalized into standardized advantages:

$$a_i = \frac{r_i - \text{mean}(\{r_j\}_{j=1}^G)}{\text{std}(\{r_j\}_{j=1}^G)}. \quad (1)$$

This allows the model to reinforce candidates that perform better than the group average, while discouraging weaker ones.

The policy parameters θ are updated by maximizing the GRPO objective:

$$\begin{aligned} \mathcal{J}_{GRPO}(\theta) = \mathbb{E}_{O \sim \pi_{\theta_{\text{old}}}} \left[\frac{1}{G} \sum_{o_i \in O} \min \left(\frac{\pi_{\theta}(o_i)}{\pi_{\theta_{\text{old}}}(o_i)} a_i, \right. \right. \\ \left. \left. \text{clip} \left(\frac{\pi_{\theta}(o_i)}{\pi_{\theta_{\text{old}}}(o_i)}, 1 - \epsilon, 1 + \epsilon \right) a_i \right) \right. \\ \left. - \beta D_{KL}(\pi_{\theta} \parallel \pi_{ref}) \right], \end{aligned} \quad (2)$$

where the clipping stabilizes training by limiting the update ratio to a range defined by ϵ , and the Kullback–Leibler (KL) divergence penalty term $D_{KL}(\pi_{\theta} \parallel \pi_{ref})$ (weighted by β) prevents the LVLM from deviating excessively from the reference model π_{ref} (typically the initialization checkpoint).

In this way, GRPO directly aligns the LVLM’s prompt generation policy with downstream segmentation performance: the LVLM progressively learns to generate bounding boxes and points that maximize IoU after execution by SAM2, without requiring any handcrafted prompt supervision.

3.2.2. Result-Oriented Reward Function

Our reward function provides direct supervision from the final segmentation result. For each output o_i , the total reward is defined as:

$$R(o_i) = \lambda_1 R_{format}(o_i) + \lambda_2 R_{IoU}(o_i), \quad (3)$$

where λ_1 and λ_2 balance the contributions of the two components.

Format reward R_{format} ensures the output is syntactically valid: it checks both the correct use of the `<think>/<answer>` tags and the validity of the JSON object. This guarantees that the generated prompts can always be parsed by the segmentation engine.

Segmentation reward R_{IoU} measures the IoU between the predicted mask M_{pred} (produced by SAM2) and the ground-truth mask M_{gt} . In empty-target scenarios, R_{IoU} is set to 1 if the model outputs an empty list and 0 otherwise. This direct IoU feedback aligns prompt generation with final segmentation performance, reinforcing strategies that improve execution outcomes.

3.2.3. Prompting Strategy for Tractability

Exploring both prompt combinations (types and numbers) and geometries (positions and sizes) would create an intractably large action space. To simplify the learning problem while preserving generality, we constrain the prompt set to a universally

effective configuration for RS: one bounding box and two positive points per instance. This design allows the LVLM to focus its optimization on spatial placement and scale, which are the most critical factors for accurate segmentation. By fixing the combination and learning only the geometry, GRPO training remains efficient and stable while still enabling diverse prompting strategies to emerge.

4. Experiments and Results

4.1. Experimental Settings

The experimental setup is described in three parts, covering datasets, evaluation metrics, and implementation details to ensure reproducibility and fair comparison.

4.1.1. Datasets

The reasoning segmentation task is evaluated on the EarthReason dataset (Li et al., 2025), currently the only publicly available benchmark for remote sensing reasoning segmentation. EarthReason contains 5,434 images across 28 categories, with the official split consisting of 2,731 training, 1,135 validation, and 1,928 test samples. These subsets include 60, 20, and 39 empty-target cases, respectively, which are critical for evaluating rejection capability. The provided ground-truth masks served as supervision during training and evaluation.

To further examine whether a model trained for reasoning segmentation can generalize to explicit referential grounding, a zero-shot transfer evaluation was performed. Specifically, the models trained solely on the EarthReason training set were directly applied to the test sets of three referring segmentation benchmarks, including RRSIS-D (Liu et al., 2024a), RIS-Bench (Dong et al., 2024), and RefSegRS (Yuan et al., 2024), without any additional fine-tuning. The RRSIS-D test set contains 3,481 samples across 20 categories, the RISBench test set includes 16,158 samples covering 26 categories, and the RefSegRS test set comprises 1,817 samples across 20 categories.

It is important to clarify the difference in annotation granularity between reasoning and referring segmentation datasets. The EarthReason dataset adopts *semantic-level masks*, in contrast to the instance-level masks used in most referring segmentation benchmarks. A semantic-level mask corresponds to a semantically coherent concept such as “greenhouse” or “residential area,” which may include multiple spatially disjoint regions that share the same functional or visual meaning. Unlike instance-level annotations that delineate individual objects, semantic-level masks emphasize semantic consistency rather than spatial continuity, aligning with the nature of reasoning segmentation where the target concept is often defined by function or context rather than by a single geometric instance.

4.1.2. Evaluation Metrics

Following prior works (Kazemzadeh et al., 2014; Yu et al., 2016; Lai et al., 2024), segmentation performance was measured using generalized Intersection-over-Union (gIoU) and cumulative Intersection-over-Union (cIoU). For a predicted mask M_{pred}

and ground-truth mask M_{gt} , with N denoting the total number of samples, gIoU is defined as:

$$gIoU = \frac{1}{N} \sum_{i=1}^N \frac{|M_{pred} \cap M_{gt}|}{|M_{pred} \cup M_{gt}|}, \quad (4)$$

and cIoU is defined as:

$$cIoU = \frac{\sum_{i=1}^N |M_{pred} \cap M_{gt}|}{\sum_{i=1}^N |M_{pred} \cup M_{gt}|}. \quad (5)$$

The gIoU reflects per-sample segmentation quality, while cIoU aggregates intersection-over-union performance across the dataset.

For the referring segmentation experiments, we additionally report P@0.5, which measures the proportion of test samples whose IoU between the predicted mask and the ground truth exceeds a threshold of 0.5:

$$P@0.5 = \frac{1}{N} \sum_{i=1}^N \mathbb{I}\left(\frac{|M_{pred} \cap M_{gt}|}{|M_{pred} \cup M_{gt}|} > 0.5\right), \quad (6)$$

where $\mathbb{I}(\cdot)$ is the indicator function. This metric reflects the model’s ability to produce accurate and confident segmentations that meet a minimum overlap threshold with the ground-truth region.

4.1.3. Implementation Details

The framework was implemented in PyTorch with DeepSpeed (Rasley et al., 2020). Qwen-2.5-VL-3B (Bai et al., 2025) was adopted as the default LVLM prompter, and a frozen SAM2-Small (Ravi et al., 2024) was used as the default segmentation module. All models were trained with bf16 precision. Input images were resized to 840×840 pixels to match the architectural requirement of Qwen-2.5-VL’s vision encoder, which processes images in 14×14 patches and requires dimensions divisible by 28.

Optimization employed AdamW (Loshchilov and Hutter, 2017) with a learning rate of 1×10^{-6} , no weight decay, and a total batch size of 16. The hyperparameters in Eq. 3 were set to $\lambda_1 = 1$ and $\lambda_2 = 2$, emphasizing the segmentation reward as the dominant signal for policy optimization. For GRPO training, the number of generations per sample was set to $G = 16$ to encourage exploration of the prompt space, and the KL divergence coefficient (β in Eq. 2) was set to 10^{-3} . All experiments were conducted on four NVIDIA A800 GPUs (80 GB memory each). The implementation was built upon the open-source VLM-R1 framework (Shen et al., 2025).

4.2. Reasoning Segmentation Results

The main results on the EarthReason dataset (Li et al., 2025) are summarized in Table 1. Following the experimental protocol of SegEarth-R1 (Li et al., 2025), the reference model introduced alongside EarthReason, all methods were trained exclusively on the official training split to ensure fair comparison.

For clarity, we categorize existing approaches into two main families. (1) End-to-end reasoning–segmentation models jointly

optimize reasoning and segmentation within a unified architecture by fine-tuning the mask decoder together with the vision–language backbone (e.g., LISA (Lai et al., 2024), PixelLM (Ren et al., 2024b), PSALM (Zhang et al., 2025), SegEarth-R1 (Li et al., 2025)). (2) Decoupled LVLM–SAM frameworks explicitly separate reasoning and segmentation into two modules: an LVLM that interprets the query and generates geometric prompts, and a frozen SAM-based executor that produces segmentation masks (e.g., Seg-Zero (Liu et al., 2025a), VisionReasoner (Liu et al., 2025b), RemoteReasoner (Yao et al., 2025b), and our proposed Think2Seg-RS).

To evaluate Seg-Zero (Liu et al., 2025a) and its successor VisionReasoner (Liu et al., 2025b) on remote sensing imagery, we adapted their training pipelines to EarthReason. Both methods were originally designed for natural image datasets such as RefCOCOg (Yu et al., 2016), which provide instance-level masks enabling direct generation of pseudo box–point supervision. In contrast, EarthReason supplies only a single semantic-level binary mask for each image, sometimes covering several spatially distinct objects (e.g., clustered storage tanks in Fig. 3). To reproduce Seg-Zero, we followed its original approach by deriving one tight bounding box and two interior points from the entire mask. For VisionReasoner, we first decomposed each semantic-level mask into sub-instances by clustering foreground pixels using DBSCAN (Ester et al., 1996), then generated a separate box–point pair for each cluster. Both reproductions were trained and evaluated under identical settings.

4.2.1. End-to-End vs. Decoupled

Across both validation and test splits, decoupled frameworks consistently outperform end-to-end counterparts. Although the mask decoder remains frozen, the LVLM–SAM family (including RemoteReasoner and our model) benefits from three key factors: (i) SAM2’s strong zero-shot segmentation prior learned from large-scale pretraining, (ii) a clean division between high-level language reasoning and low-level pixel execution, and (iii) reinforcement learning that directly ties prompt quality to downstream segmentation accuracy. In contrast, end-to-end models must align compressed LVLM embeddings with a learnable decoder, which often creates optimization bottlenecks and limits generalization when facing open-ended, free-form natural language queries.

4.2.2. Against End-to-End SFT Methods

Relative to the strongest end-to-end baseline (SegEarth-R1), Think2Seg-RS (7B) achieves significant improvements of +2.98 gIoU and +7.58 cIoU on the test set. Even the lighter 3B variant outperforms SegEarth-R1 by +0.34 gIoU and +5.88 cIoU, demonstrating that a reinforcement learning–optimized prompting policy is more data-efficient and scalable than training a task-specific decoder.

4.2.3. Comparison Within Decoupled Methods

Within the decoupled family, we compare four representative frameworks: Seg-Zero, VisionReasoner, RemoteReasoner, and our Think2Seg-RS. As shown in Table 1, RemoteReasoner (Yao et al., 2025b) is the strongest published baseline, while our

Table 1: Comparison of reasoning segmentation results on the EarthReason dataset

Method	Model	Validation		Test	
		gIoU	cIoU	gIoU	cIoU
<i>End-to-End Reasoning-Segmentation Models</i>					
LISA* (Lai et al., 2024)	CLIP-L (304M) + Vicuna-7B	61.04	57.39	60.88	59.10
PixelLM* (Ren et al., 2024b)	CLIP-L (304M) + Vicuna-7B	57.94	57.79	60.01	59.22
PSALM* (Zhang et al., 2025)	Swin-B (88M) + Phi-1.5-1.3B	66.61	62.03	68.30	64.61
SegEarth-R1 (Li et al., 2025)	Swin-B (88M) + Phi-1.5-1.3B	68.60	64.13	70.75	68.25
<i>Decoupled LVLM-SAM Frameworks</i>					
Seg-Zero [†] (Liu et al., 2025a)	Qwen-2.5-VL-7B + SAM2-Large	63.00	61.93	63.16	62.76
VisionReasoner [†] (Liu et al., 2025b)	Qwen-2.5-VL-7B + SAM2-Large	66.50	67.98	67.17	65.29
RemoteReasoner (Yao et al., 2025b)	Qwen-2.5-VL-7B + SAM2 [‡]	69.02	67.80	70.96	69.13
Think2Seg-RS (ours)	Qwen-2.5-VL-3B + SAM2-Small	69.30	71.28	71.09	74.13
Think2Seg-RS (ours)	Qwen-2.5-VL-7B + SAM2-Small	72.46	73.62	73.73	75.83

Note: * denotes results reproduced by the SegEarth-R1 paper (Li et al., 2025); [†] indicates results reproduced by us on the EarthReason dataset; [‡] indicates that the SAM2 version was not specified in the RemoteReasoner paper (Yao et al., 2025b).

Think2Seg-RS (7B) further pushes the state of the art to 73.73 gIoU and 75.83 cIoU on the test set, surpassing RemoteReasoner by +2.77 and +6.70 points, respectively. The smaller 3B model also performs competitively, achieving 71.09 gIoU and 74.13 cIoU, comparable to RemoteReasoner in gIoU and clearly superior in cIoU (+5.00). The pronounced cIoU gain suggests that Think2Seg-RS produces more globally coherent and complete segmentation masks, benefiting from mask-level reinforcement signals instead of instance-level pseudo supervision. While gIoU primarily captures per-instance geometric accuracy, cIoU reflects overall coverage and cross-scene consistency, highlighting that our mask-based optimization improves both spatial completeness and prediction stability across diverse samples.

The performance gap among decoupled methods can be largely attributed to differences in supervision and reward design. Both Seg-Zero and VisionReasoner rely on pseudo instance-level box–point supervision, which is unavailable in EarthReason. To reproduce these methods, we derived one bounding box and two points from each semantic-level mask for Seg-Zero, and applied DBSCAN to decompose masks into sub-instances before generating box–point pairs for VisionReasoner. However, both strategies inevitably introduce noisy geometric supervision due to the lack of true instance annotations, leading to degraded performance. RemoteReasoner extends this idea to remote sensing by converting masks into boxes through a mask-to-box procedure and adopting a composite reward that balances bounding box IoU, count, and format validity. This design alleviates annotation noise and aligns policy learning with object separation and structural correctness, explaining its superior performance relative to our Seg-Zero and VisionReasoner reproductions.

In contrast, Think2Seg-RS eliminates the need for any pseudo instance supervision. The LVLM is optimized directly through mask-level reinforcement using only the final segmentation quality as feedback. This mask-only optimization avoids the bias introduced by synthetic boxes and points and allows the model to explore a wider range of prompting strategies. Consequently, Think2Seg-RS achieves higher scene-level completeness and

more accurate boundary delineation, as reflected in its substantial cIoU improvement.

4.2.4. Qualitative Behavior

Figure 3 presents representative examples illustrating the reasoning traces and geometric prompting behaviors of Think2Seg-RS across diverse remote sensing scenarios. In each case, the model first verbalizes its reasoning process in the `<think>` stage, where it interprets the query, identifies relevant visual cues, and infers the semantic and spatial scope of the target, before generating structured prompts in the `<answer>` stage.

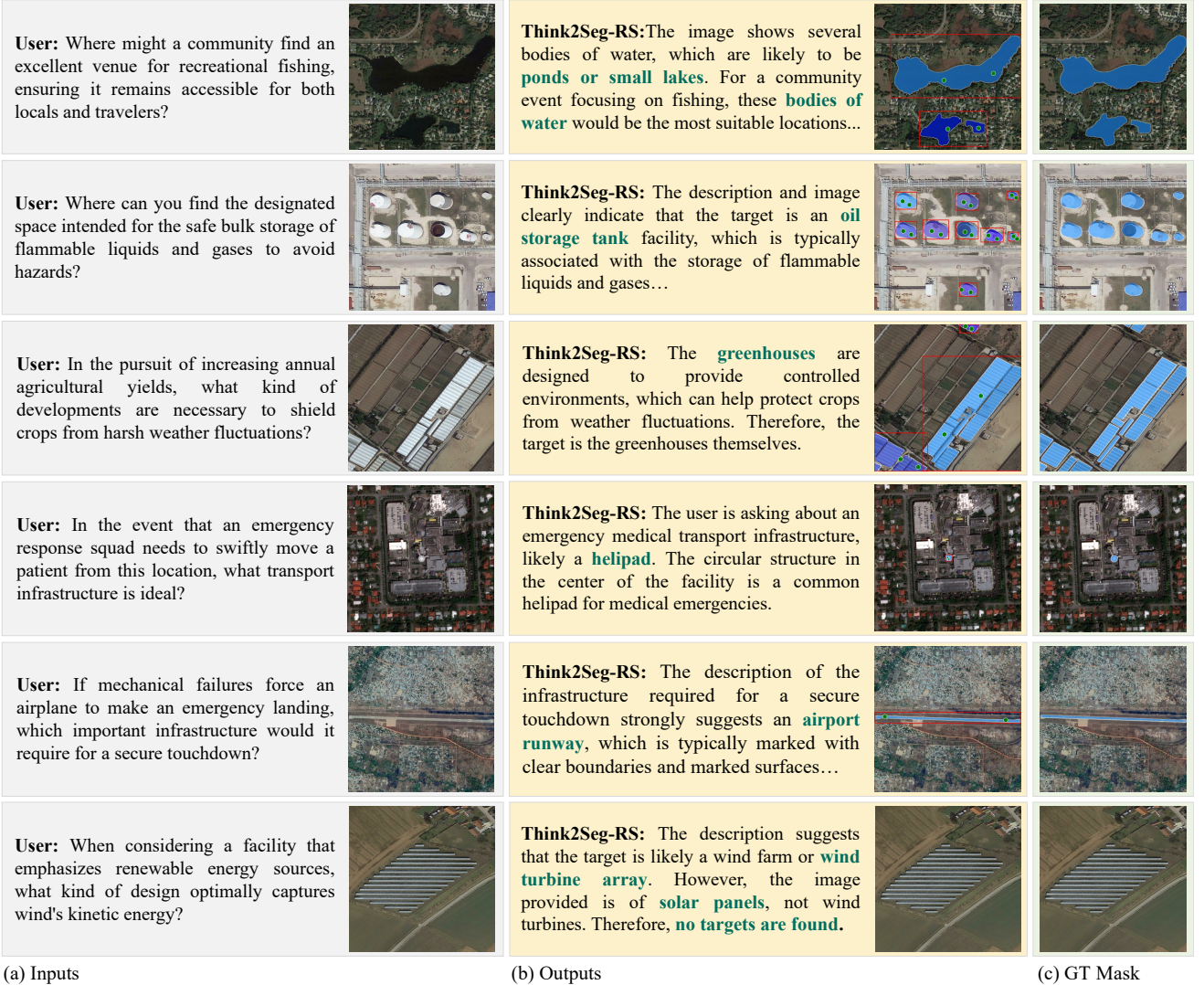
In the first example, responding to a query about a recreational fishing venue, the model correctly identifies the target as “bodies of water”. It then generates precise box and points for the single large waterbody, and an encompassing box that groups the two smaller, adjacent waterbodies, each marked by a distinct point, showcasing its flexible prompts for SAM.

The second example, depicting an oil storage facility, highlights the model’s handling of multi-instance regions. Its reasoning connects “storage of flammable liquids” with “oil storage tanks,” producing distinct boxes for each tank even though the ground-truth annotation merges them into one mask.

In the third row, featuring a greenhouse complex, Think2Seg-RS reasons that “the greenhouses are designed to provide controlled environments” and demonstrates a flexible grouping strategy. It correctly recognizes that the target consists of spatially separate clusters and, accordingly, partitions them into three subgroups for segmentation. This reveals its ability to adapt its prompting strategy to the target’s spatial distribution.

The fourth example showcases robust localization of a small yet semantically critical object in a dense urban environment. The model reasons that a “helipad” is a circular structure for medical emergencies and generates a tightly fitted prompt around the correct feature.

In the fifth example, the model correctly interprets “infrastructure required for a secure touchdown” as an airport runway and generates elongated, axis-aligned prompts that precisely align with the target’s linear structure.



(a) Inputs

(b) Outputs

(c) GT Mask

Fig. 3: Qualitative results of Think2Seg-RS on the EarthReason dataset. (a) Inputs, including the user query and corresponding remote sensing image. (b) Model outputs, comprising the LViM’s reasoning text from the `<think>` stage, the generated geometric prompts (bounding boxes in red and positive points in green), and the resulting segmentation mask predicted by SAM2. (c) Ground-truth (GT) mask for reference.

Finally, the last example illustrates reliable negative reasoning. The model correctly rejects an invalid instruction, reasoning that “the image provided is of solar panels, not wind turbines,” and outputs an empty prompt list, showcasing its ability to recognize semantic mismatches and abstain from false predictions. This rejection behavior will be further analyzed in Subsection 4.3.

Overall, these qualitative examples demonstrate that our Think2Seg-RS integrates interpretable reasoning with precise spatial execution. The textual reasoning traces provide insight into the decision process, while the geometric prompts reveal structured spatial understanding, together forming a coherent reasoning-to-execution pipeline capable of handling diverse structures, implicit semantics, and open-ended instructions in remote sensing imagery.

For a more comprehensive evaluation, the appendix presents additional examples (Fig. Appendix B.1) and representative

failure cases (Fig. Appendix B.2) of Think2Seg-RS on the EarthReason dataset.

4.3. Analysis of Rejection Capability

RS imagery often features complex, cluttered backgrounds and large intra-class variance, making it common for the queried object to be absent from a given scene. An effective reasoning-segmentation model must therefore recognize such absence and avoid hallucinating false positives, which can lead to misleading downstream analysis. To quantitatively assess this ability, we evaluated the rejection performance of Think2Seg-RS on the validation and test sets of the EarthReason dataset. Since the Seg-Zero framework lacks an inherent rejection mechanism, we compare our Think2Seg-RS (3B and 7B) with SegEarth-R1, which includes this capability.

As summarized in Table 2, our framework exhibits a substantially stronger rejection capability. The SegEarth-R1 baseline tends to over-segment ambiguous scenes, producing false

Table 2: Comparison of rejection capability on the EarthReason dataset

Method	Validation (20 cases)		Test (39 cases)	
	TRUE	FALSE	TRUE	FALSE
SegEarth-R1	6 (30.0)	14 (70.0)	9 (23.1)	30 (76.9)
Think2Seg-RS-3B	9 (45.0)	11 (55.0)	19 (48.7)	20 (51.3)
Think2Seg-RS-7B	12 (60.0)	8 (40.0)	24 (61.5)	15 (38.5)

Note: TRUE and FALSE denote the number (%) of correctly and incorrectly classified empty-target samples, respectively.

positives in most empty-target cases. In contrast, both variants of Think2Seg-RS achieve marked improvements. The 3B model more than doubles the number of correct rejections on the test set, while the 7B model further enhances this ability, correctly identifying 24 of 39 empty-target samples. This scaling trend underscores that a more capable LVLM, trained under our result-oriented reinforcement objective, develops a refined understanding of absence conditions. As illustrated in the last row of Figure 3, the model’s rejection is not arbitrary. It provides explicit reasoning such as “no targets are found,” offering interpretable and trustworthy feedback.

4.4. Generalization on Referring Expression Segmentation

Reasoning segmentation and referring expression segmentation are closely related but differ fundamentally in task formulation. The former requires implicit and compositional reasoning that links textual descriptions to semantic regions through multi-step inference, whereas the latter involves explicit visual grounding of a directly mentioned target. Intuitively, a model capable of performing reasoning segmentation should, in principle, possess the necessary understanding to handle the simpler referring task. To verify this assumption and examine whether reasoning-trained models can generalize to explicit referential grounding, we conducted a challenging zero-shot transfer experiment.

Specifically, the models optimized for the reasoning segmentation task on the EarthReason dataset (Li et al., 2025) were subsequently tested on three referring segmentation benchmarks, including RRSIS-D (Liu et al., 2024a), RISBench (Dong et al., 2024), and RefSegRS (Yuan et al., 2024), to evaluate their zero-shot transfer capability without any additional fine-tuning. This setting jointly tests cross-dataset transfer (different visual distributions) and cross-task transfer (from reasoning to referring), providing a rigorous assessment of the model’s reasoning-to-referring adaptability.

4.4.1. Results and Observations

The results, summarized in Table 3, present a comprehensive comparison across multiple model paradigms. To establish reference points, we first include two direct zero-shot baselines: Qwen-2.5-VL-3B+SAM2 and Qwen-2.5-VL-7B+SAM2, which use the off-the-shelf LVLMs and SAM executor without any training on EarthReason or the referring datasets. These models demonstrate the inherent capability of general-purpose LVLMs to perform coarse referring segmentation, yet their performance remains modest across all datasets, confirming that task-specific adaptation is essential for robust grounding in the RS domain.

Next, we evaluate SegEarth-R1 (Li et al., 2025), reproduced by us on EarthReason, which represents an end-to-end SFT paradigm that jointly fine-tunes the reasoning and segmentation components. Although effective on the training dataset (see Table 1), SegEarth-R1 performs poorly under zero-shot transfer. This sharp degradation highlights the limited generalizability of SFT-based models, which tend to overfit to dataset-specific visual-text priors and struggle to adapt when the data distribution or task formulation shifts.

Among the decoupled frameworks, Seg-Zero (Liu et al., 2025a) and VisionReasoner (Liu et al., 2025b), both reproduced using our EarthReason-trained LVLM-SAM pipeline, show considerably higher transferability. Their instance-level box-point supervision enables more localized and fine-grained grounding, yielding superior gIoU and cIoU on RRSIS-D and RISBench. The RemoteReasoner (Yao et al., 2025b) results, reported from its original paper, further improve upon these baselines via a refined mask-to-box generation and composite reward scheme, achieving 50.97 gIoU and 54.29 P@0.5 on RRSIS-D.

In contrast, our Think2Seg-RS models exhibit a markedly different behavior. While demonstrating strong semantic-level reasoning capability, they underperform instance-oriented methods on RRSIS-D and RISBench. However, on the RefSegRS benchmark, Think2Seg-RS attains the best overall performance among all models (15.53 gIoU, 17.75 cIoU, and 7.43 P@0.5).

4.4.2. Analysis and Interpretation

The cross-task generalization behavior can be explained by the intrinsic differences in both dataset characteristics and methodological design.

Dataset Characteristics. In our experimental setting, the models are fine-tuned on the EarthReason dataset for reasoning segmentation and then transferred to three referring segmentation benchmarks: RRSIS-D, RISBench, and RefSegRS. These four datasets, in our opinion, collectively span a continuum from explicit referring to implicit reasoning, differing in both semantic granularity and geometric complexity.

RRSIS-D is a representative instance-level benchmark where each query uniquely identifies a single target instance, which often presents vast variations in scale and orientation. Its queries are therefore explicit, describing geometric and visual attributes (e.g., “the gray rounded storage tank in the middle”). RISBench extends this instance-level paradigm with larger scale and linguistic diversity. It introduces longer and attribute-rich expressions with relational cues (e.g., “the black vehicle at the middle-right edge of the image is partially hidden behind the house”).

RefSegRS represents the early stage of referring segmentation task in remote sensing with a semantic-level paradigm. The task here is to segment all instances matching a semantic description, rather than a single object. Its expressions, generated from templates, are concise and specify an object category with an optional spatial context (e.g., “building along the road”). This one-to-many grounding paradigm aligns with tasks requiring holistic scene understanding rather than single-object localization.

Table 3: Zero-shot evaluation results on the referring segmentation benchmarks RRSIS-D, RISBench, and RefSegRS

Method	RRSIS-D			RISBench			RefSegRS		
	gIoU	cIoU	P@0.5	gIoU	cIoU	P@0.5	gIoU	cIoU	P@0.5
Qwen-2.5-VL-3B+SAM2	14.87	15.86	12.94	15.85	12.80	15.58	4.18	6.23	0.74
Qwen-2.5-VL-7B+SAM2	28.14	30.45	37.06	26.30	25.76	31.15	5.16	8.29	3.09
SegEarth-R1* (Li et al., 2025)	26.34	26.80	25.05	15.82	16.04	13.65	1.92	3.93	0.28
Seg-Zero* (Liu et al., 2025a)	43.70	47.68	45.83	41.25	37.36	41.56	10.08	12.59	3.69
VisionReasoner* (Liu et al., 2025a)	49.39	54.99	53.69	51.62	46.98	54.87	11.15	12.32	4.46
RemoteReasoner (Yao et al., 2025b)	50.97	-	54.29	-	-	-	-	-	-
Think2Seg-RS-3B (ours)	43.42	48.66	45.10	40.04	36.49	39.37	14.91	16.46	6.60
Think2Seg-RS-7B (ours)	47.97	54.30	51.66	47.72	44.18	50.00	15.53	17.75	7.43

Note: * indicates models reproduced by us on the EarthReason dataset.

EarthReason generalizes the task into implicit semantic-level reasoning. Each query involves contextual or causal inference beyond direct visual naming. The conceptual landscape defined by these benchmarks illustrates a gradual shift along both visual and linguistic dimensions. This continuum transitions from geometric localization and attribute grounding to semantic abstraction and contextual reasoning, and defines the semantic–geometric landscape for our cross-dataset analysis.

Methodological Design. The performance gap across datasets is also driven by the fundamental differences in model supervision. Think2Seg-RS is trained under a mask-only reinforcement learning paradigm, where the LVLM is optimized with a result-oriented reward signal centered on the final mask IoU. This learning scheme equips the model with strong *semantic-level* reasoning and generalization abilities without relying on geometric priors such as bounding boxes or points. However, the absence of instance-level geometric priors fosters an inductive bias toward holistic semantic matching over pinpoint instance grounding. In contrast, VisionReasoner and RemoteReasoner both adopt explicit *instance-level* pseudo supervision, a strategy reliant on the costly generation of box–point prompts as spatial priors for each sample. This supervision strategy embeds a strong bias for instance-aware alignment, which directly matches the single-object localization objective of the RRSIS-D and RISBench benchmarks.

Interpretation. Consequently, Think2Seg-RS achieves the best performance on *semantic-level* datasets (EarthReason and zero-shot on RefSegRS), where semantic consistency and contextual reasoning dominate. Its policy learning directly aligns language-driven reasoning with holistic regional segmentation, producing coherent masks that match the implicit or explicit semantic intent of the query. However, when transferred to *instance-level* referring expression segmentation benchmarks (zero-shot on RRSIS-D, RISBench), the model’s inductive bias toward holistic semantic matching conflicts with the core task of pinpointing a single instance, resulting in lower precision than models trained with instance-aware geometric priors.

These observed results therefore reflect not a weakness but a difference in *inductive bias*: the mask-only signal nurtures a bias for holistic semantic understanding, whereas the box–point

supervision signal fosters a strong bias toward precise geometric localization. This divergence highlights a fundamental trade-off: Think2Seg-RS prioritizes semantic abstraction and context reasoning, while VisionReasoner and RemoteReasoner specialize in geometric grounding and fine spatial alignment.

4.5. Ablation Study

We conducted three ablation studies to evaluate the individual contributions of key components in the Think2Seg-RS framework. Specifically, we examined the influence of the LVLM prompter, the model size of SAM2, and various prompt combination strategies. All experiments were carried out on the EarthReason dataset, using Qwen-2.5-VL-3B as the default prompter and SAM2-Small as the default segmenter unless otherwise specified.

4.5.1. Ablation on LVLM Prompter

The effect of different LVLM prompters and model sizes on the performance of Think2Seg-RS was evaluated. As presented in Table 4, multiple LVLM families and scales were compared, including LLaVA-1.5-7B (Liu et al., 2023), the Qwen-2.5-VL series (3B and 7B) (Bai et al., 2025), and the InternVL3 series (2B and 8B) (Zhu et al., 2025). All experiments in this study employed SAM2-Small as the segmenter to ensure a consistent evaluation of the LVLM prompter’s influence. For the InternVL3 models, input images were resized to 896×896 pixels to match their default configuration.

Table 4: Ablation study on LVLM prompter and model size

LVLM	Validation		Test	
	gIoU	cIoU	gIoU	cIoU
LLaVA-1.5-7B	38.60	35.84	39.26	36.94
InternVL3-2B	64.59	64.53	66.03	66.96
InternVL3-8B	72.16	71.91	73.24	73.13
Qwen-2.5-VL-3B	69.30	71.28	71.09	74.13
Qwen-2.5-VL-7B	72.46	73.62	73.73	75.83

The results indicate that Think2Seg-RS achieves consistently strong performance when paired with recent high-capacity LVLMs, particularly the Qwen-2.5-VL and InternVL3 series.

Among them, Qwen-2.5-VL-7B attains the overall best results on both validation and test sets, while InternVL3-8B also demonstrates comparable performance. A clear scaling trend is observed, where larger models within the same family outperform their smaller counterparts, suggesting that reasoning segmentation performance directly benefits from the enhanced reasoning and perception capabilities of larger-scale LVLMs.

It is also notable that LLaVA-1.5-7B performs significantly worse than the other LVLMs. This performance gap can be attributed to the architectural and training differences between LLaVA and other multimodal large language models such as Qwen-2.5-VL and InternVL3. LLaVA-1.5 was primarily optimized for visual dialogue and image captioning on natural images, relying on a limited visual encoder and a smaller, instruction-tuned dataset. In contrast, Qwen-2.5-VL and InternVL3 were trained with high-resolution perception and stronger multimodal alignment, making them substantially more capable of handling the complex spatial reasoning and semantic grounding required in reasoning segmentation tasks. Consequently, the results highlight the importance of both large-scale reasoning pretraining and fine-grained multimodal alignment for achieving high performance in Think2Seg-RS.

4.5.2. Ablation on the Model Scale of SAM2

To examine the influence of the segmentation backbone on overall performance, the impact of the SAM2 model scale was systematically evaluated. Four variants, including SAM2-Tiny, SAM2-Small, SAM2-Base-plus, and SAM2-Large, were compared while keeping all other components fixed. Unlike the LVLM ablation study, where larger models consistently improved reasoning capability, our results reveal a counterintuitive trend: increasing the size of SAM2 does not necessarily lead to better performance (Table 5). Among the four variants, SAM2-Small achieves the best trade-off between segmentation performance and computational efficiency, and is therefore adopted as the default segmenter in Think2Seg-RS.

Table 5: Ablation study on the model scale of SAM2

SAM2 Size	Validation		Test	
	gIoU	cIoU	gIoU	cIoU
Tiny (38.9M)	69.36	71.24	70.62	73.94
Small (46.0M)	69.30	71.28	71.09	74.13
Base-plus (88.8M)	69.50	70.38	70.78	72.84
Large (224.4M)	68.04	69.45	70.43	72.39

This phenomenon arises from the distinct interaction between segmentation granularity and the *semantic-level annotation paradigm*. Larger SAM2 variants, such as SAM2-Base-plus and SAM2-Large, possess fine-grained sensitivity that is advantageous for instance-level or natural-image tasks but becomes a liability in semantic-level reasoning. These high-capacity models tend to over-segment by capturing small structural details and textural noise (e.g., variations in terrain, vegetation, or man-made substructures). As illustrated in Fig. 4, when applied to a wastewater treatment plant, the larger models attempt to delineate each tank and the negative spaces between them, resulting

in a fragmented, quasi-instance-level output that poorly aligns with the ground truth mask. Since the annotation is intentionally designed to represent the entire facility as a single coherent polygon, such excessive detail introduces a semantic mismatch that lowers the IoU score.

Conversely, smaller variants like SAM2-Tiny and SAM2-Small exhibit an implicit regularization effect due to their constrained capacity. They smooth over fine textures and small gaps, producing spatially coherent masks that better match the coarse, semantic-level labeling prevalent in remote sensing. This alignment between model behavior and annotation granularity explains why smaller SAM2 variants outperform larger ones in reasoning segmentation. In essence, the optimal model scale is not absolute but depends on the desired level of semantic abstraction and the annotation style of the target domain.

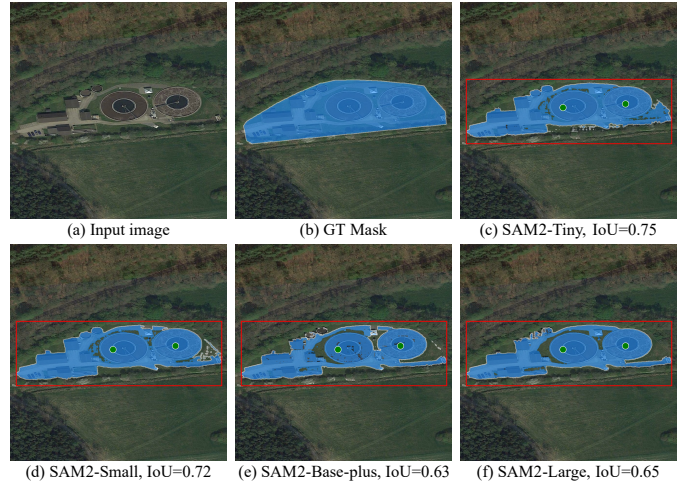


Fig. 4: Effect of SAM2 model scale on semantic-level segmentation. (a) Input image and (b) corresponding ground-truth (GT) mask illustrate a semantic-level annotation where the entire wastewater treatment plant is represented as one coherent polygon. Outputs from four SAM2 variants, namely (c) Tiny, (d) Small, (e) Base-plus, and (f) Large, show that larger models generate over-detailed, fragmented masks misaligned with the coarse annotation style, resulting in lower IoU scores. In contrast, smaller variants (Tiny and Small) produce smoother, spatially coherent masks that better match the semantic-level ground truth, achieving higher IoU values.

4.5.3. Ablation on Prompt Combination

SAM is inherently sensitive to the type and configuration of input prompts. Since our Think2Seg-RS framework freezes the SAM segmenter and relies solely on the LVLM to generate prompts, the prompt combination becomes a critical factor that determines the final segmentation quality. To quantitatively and qualitatively understand this sensitivity, we conducted an ablation study on different prompt combinations, evaluating five configurations: (1) bounding box only, (2) two positive points only, (3) bounding box with two positive points, (4) bounding box with four positive points, and (5) bounding box with two positive points plus two negative points.

The quantitative results summarized in Table 6, together with qualitative examples in Fig. 5, provide a comprehensive view of the model’s behavior under different prompt combinations. A

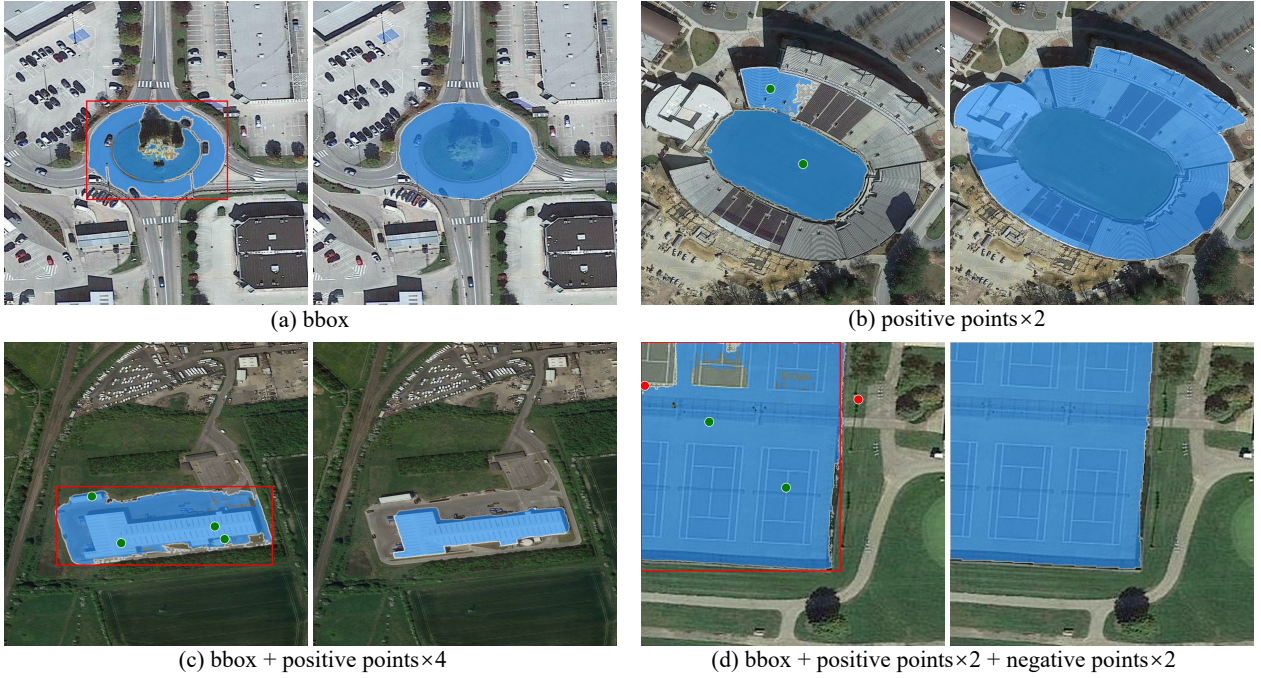


Fig. 5: Qualitative analysis of prompting combination strategies for SAM. Each pair displays the input image with LVLM generated prompts and the resulting segmentation mask (left, bounding boxes in red, positive points in green, negative points in red) and the ground-truth mask (right).

Table 6: Ablation Study on SAM Prompt Combination

Prompt Combination	val		test	
	gIoU	cIoU	gIoU	cIoU
bbox	67.61	69.68	68.27	70.95
pos_points×2	56.15	53.63	56.01	53.78
bbox + pos_points×2	69.30	71.28	71.09	74.13
bbox + pos_points×4	67.31	69.54	69.18	72.45
bbox + pos_points×2 + neg_points×2	66.36	68.91	68.21	72.16

single bounding box offers coarse localization but often covers multiple semantic regions. Without explicit semantic cues, the frozen SAM focuses on the dominant texture (e.g., pavement) and omits heterogeneous content (e.g., vegetation or shadows), producing an incomplete segmentation (Fig. 5a). Using only two positive points produces incomplete masks, as the limited cues cannot represent the diverse visual and semantic patterns within large or complex targets (Fig. 5b). Combining one bounding box with two positive points achieves the best overall performance by balancing semantic coverage and geometric constraint. The bounding box provides a global spatial prior, while the two positive points help disambiguate heterogeneous regions within the box, guiding SAM toward the intended semantic scope. This configuration serves as the default setting in Think2Seg-RS and consistently produces coherent regional masks across diverse scenes (see Fig. 3).

However, increasing the number of positive points to four does not further improve the results (Fig. 5c). In many cases, these additional points fall into semantically diverse subregions within the same bounding box, such as rooftops, shadows, or adjacent ground textures, which causes the frozen SAM to merge

inconsistent cues. This leads to overextended or irregular masks that blur the intended semantic scope. Introducing negative points further degrades performance (Fig. 5d). Unlike positive cues, which highlight coherent semantic areas, negative regions in aerial imagery are inherently heterogeneous, encompassing materials and textures such as vegetation, concrete, water, or asphalt. Such diversity prevents the LVLM from learning a stable placement strategy for negative prompts, and their inconsistent signals often conflict with positive cues. As a result, the generated masks become fragmented or distorted, reflecting the difficulty of defining uniform “non-target” semantics in high-resolution remote sensing scenes.

This observed sensitivity reflects a deeper mechanism of the decoupled LVLM–SAM architecture. Since the segmenter is frozen, all semantic information must be conveyed through spatial prompts generated by the LVLM. Consequently, prompt configuration directly determines how effectively high-level textual semantics are translated into low-level spatial cues. When the generated prompts are semantically well aligned with the target regions, the interaction between the LVLM and the frozen SAM becomes more efficient, enabling SAM to produce coherent and complete regional masks. Conversely, misaligned or redundant prompts distort this semantic mapping, leading to either under-segmentation or overextension. These results highlight that the effectiveness of decoupled prompting depends not only on the reasoning ability of the LVLM but also on how efficiently the prompt space encodes semantic intent. This interplay between language-driven semantics and frozen visual priors defines the core behavior of the Think2Seg-RS framework.

5. Discussion

Scope and positioning. Think2Seg-RS reframes reasoning segmentation in remote sensing as a process of learning to prompt a frozen segmenter. By optimizing an LVLM through a lightweight, mask-only GRPO signal, the framework transfers high-level reasoning into geometric prompts that SAM2 can reliably execute. Here we discuss the broader implications of our findings, focusing on cross-task applicability, sensitivity of the prompt interface, and the interaction between segmenter capacity and annotation granularity.

Cross-task generalization and applicability domain. Our zero-shot transfer experiments revealed a consistent pattern: Think2Seg-RS generalizes strongly to *semantic-level referring tasks*, yet shows a performance gap on *instance-level* benchmarks. This outcome reflects the inductive bias of our mask-level reinforcement learning objective. Optimizing for global IoU encourages the LVLM to capture semantic coherence and scene-level completeness—traits advantageous for EarthReason and Ref-SegRS, both of which adopt semantic-level supervision. However, this formulation lacks explicit geometric priors required for instance discrimination in datasets such as RRSIS-D and RISBench, where numerous small, rotated, or adjacent targets must be individually grounded. Bridging this gap calls for light, geometry-aware extensions to the current design: orientation- and thin-structure consistency terms in the reward, an expanded prompt vocabulary including rotated boxes and line or multi-point chains, and a small amount of referring-style supervision for curriculum calibration. These augmentations would enhance instance precision while preserving the strong semantic-level generalization that characterizes Think2Seg-RS.

Prompt interface sensitivity and the role of negative points. Because the segmenter is frozen, all semantic information is conveyed through the spatial prompts generated by the LVLM. Our ablation results show that this interface performs best when balancing semantic coverage and geometric constraint (one box with two positive points), but becomes unstable when prompts are sparse, redundant, or semantically conflicting. In particular, negative points underperform not due to a design flaw, but because non-target regions in remote sensing imagery are intrinsically heterogeneous. A single “negative” cue may correspond to vegetation, roofs, asphalt, or water surfaces, making it difficult for the LVLM to learn a consistent placement strategy and often injecting contradictory signals into SAM2. Future work should focus on developing semantic-aware negative prompting, where negatives are placed on confounding look-alike regions or adversarially mined around predicted boundaries, thus improving contrastive separation between the intended target and its surrounding semantics. An adaptive prompting policy that first infers target morphology and background heterogeneity, then selects an appropriate prompt template, offers a practical route toward robustness and interpretability (see Fig. [Appendix B.3](#) for illustrative examples).

Segmenter scale versus annotation granularity. A counterintuitive but consistent observation is that smaller SAM2 variants

outperform larger ones under semantic-level supervision. High-capacity segmenters tend to overfit to high-frequency textures and microstructures, which misalign with the coarse semantic masks provided in reasoning segmentation. In contrast, compact models act as implicit regularizers, smoothing over noisy details and better capturing the primary object structures relevant to semantic-level tasks. This observation suggests a general principle for the RS domain: the capacity and inductive bias of the execution engine should match the granularity and abstraction level of the annotation. Such alignment yields better accuracy–efficiency trade-offs and avoids unnecessary scaling in large remote-sensing models.

Limitations and actionable next steps. Think2Seg-RS currently relies on a single-turn policy and a fixed prompt schema, without explicit uncertainty estimation. Several extensions are immediately actionable: (i) introducing geometry-aware rewards that incorporate orientation, skeleton, and length consistency for slender or rotated targets; (ii) adopting adaptive prompting strategies that condition the prompt template on inferred target morphology and background heterogeneity, including semantic-aware negatives; and (iii) integrating minimal calibration data that mixes limited referring-style supervision or multi-turn corrections to refine instance precision while maintaining scalability. These steps preserve the advantages of decoupling, including modularity, efficiency, and interpretability, while broadening the applicability from semantic-level reasoning toward fine-grained, instance-centric grounding.

Takeaway. The observed transfer patterns and ablation behaviors do not weaken the contribution of Think2Seg-RS; rather, they clarify its applicability domain and illuminate clear directions for extension. Mask-only GRPO equips the LVLM with a transferable prompting skill that excels in tasks emphasizing semantic coherence. By enriching the reward and prompt space with lightweight geometric priors and adaptive policies, the same decoupled formulation can be extended toward high-precision referring segmentation in instance-dense remote-sensing scenes.

6. Conclusion

In this study, we presented Think2Seg-RS, a decoupled large vision–language framework for reasoning segmentation in remote sensing. By training an LVLM prompter to guide a frozen SAM2 segmenter through geometric prompts and optimizing it with a mask-only GRPO reward, Think2Seg-RS bridges abstract semantic reasoning with concrete spatial delineation. This paradigm achieves state-of-the-art performance on the EarthReason dataset and exhibits strong zero-shot transfer to referring segmentation benchmarks, demonstrating robust cross-dataset and cross-task generalization.

Experiments further reveal that compact SAM2 variants better align with semantic-level supervision, while negative prompting remains challenging due to the heterogeneous backgrounds in aerial imagery. Overall, Think2Seg-RS provides an efficient and scalable paradigm for semantic-level reasoning segmentation and points toward future extensions in adaptive prompting,

geometry-aware rewards, and unified semantic–instance segmentation for geospatial analysis.

Declaration of Competing Interest

The authors declare that they have no known competing financial interests or personal relationships that could have appeared to influence the work reported in this paper.

Declaration of generative AI and AI-assisted technologies in the manuscript preparation process

During the preparation of this manuscript, the authors utilized ChatGPT to assist with language enhancement and improve readability. After utilizing this tool, the authors thoroughly reviewed and revised the content as necessary, and take full responsibility for the final manuscript.

Acknowledgments

This work was supported in part by the National Natural Science Foundation of China (Grant Nos. 62476205 and 62301405), and the Fundamental Research Funds for the Central Universities (Grant Nos. ZYTS25152 and ZYTS25136).

References

Azimi, S.M., Henry, C., Sommer, L., Schumann, A., Vig, E., 2019. SkyScapes – fine-grained semantic understanding of aerial scenes, in: Proceedings of the IEEE/CVF International Conference on Computer Vision, pp. 7393–7403.

Bai, S., Chen, K., Liu, X., Wang, J., Ge, W., Song, S., Dang, K., Wang, P., Wang, S., Tang, J., et al., 2025. Qwen2.5-VL technical report. arXiv preprint arXiv:2502.13923 .

Bai, Z., He, T., Mei, H., Wang, P., Gao, Z., Chen, J., Zhang, Z., Shou, M.Z., 2024. One token to seg them all: Language instructed reasoning segmentation in videos. Advances in Neural Information Processing Systems 37, 6833–6859.

Chen, K., Liu, C., Chen, H., Zhang, H., Li, W., Zou, Z., Shi, Z., 2024a. RSPrompter: Learning to prompt for remote sensing instance segmentation based on visual foundation model. IEEE Transactions on Geoscience and Remote Sensing 62, 1–17.

Chen, Y.C., Li, W.H., Sun, C., Wang, Y.C.F., Chen, C.S., 2024b. SAM4MLM: Enhance multi-modal large language model for referring expression segmentation, in: European Conference on Computer Vision, Springer. pp. 323–340.

Dong, Z., Sun, Y., Liu, T., Zuo, W., Gu, Y., 2024. Cross-modal bidirectional interaction model for referring remote sensing image segmentation. arXiv preprint arXiv:2410.08613 .

Ester, M., Kriegel, H.P., Sander, J., Xu, X., et al., 1996. A density-based algorithm for discovering clusters in large spatial databases with noise, in: Proceedings of the Second International Conference on Knowledge Discovery and Data Mining, pp. 226–231.

Guo, S., Jin, Q., Wang, H., Wang, X., Wang, Y., Xiang, S., 2019. Learnable gated convolutional neural network for semantic segmentation in remote-sensing images. Remote Sensing 11, 1922.

Kazemzadeh, S., Ordonez, V., Matten, M., Berg, T., 2014. ReferItGame: Referring to objects in photographs of natural scenes, in: Proceedings of the 2014 conference on empirical methods in natural language processing (EMNLP), pp. 787–798.

Kirillov, A., Mintun, E., Ravi, N., Mao, H., Rolland, C., Gustafson, L., Xiao, T., Whitehead, S., Berg, A.C., Lo, W.Y., et al., 2023. Segment anything, in: Proceedings of the IEEE/CVF international conference on computer vision, pp. 4015–4026.

Lai, X., Tian, Z., Chen, Y., Li, Y., Yuan, Y., Liu, S., Jia, J., 2024. LISA: Reasoning segmentation via large language model, in: Proceedings of the IEEE/CVF Conference on Computer Vision and Pattern Recognition, pp. 9579–9589.

Lan, M., Chen, C., Zhou, Y., Xu, J., Ke, Y., Wang, X., Feng, L., Zhang, W., 2025. Text4Seg: Reimagining image segmentation as text generation, in: The Thirteenth International Conference on Learning Representations. URL: <https://openreview.net/forum?id=vkakKdznFS>.

Lei, S., Xiao, X., Zhang, T., Li, H.C., Shi, Z., Zhu, Q., 2025. Exploring fine-grained image-text alignment for referring remote sensing image segmentation. IEEE Transactions on Geoscience and Remote Sensing 63, 1–11. doi:[10.1109/TGRS.2024.3522293](https://doi.org/10.1109/TGRS.2024.3522293).

Li, K., Xin, Z., Pang, L., Pang, C., Deng, Y., Yao, J., Xia, G., Meng, D., Wang, Z., Cao, X., 2025. SegEarth-R1: Geospatial pixel reasoning via large language model. arXiv preprint arXiv:2504.09644 .

Liu, H., Li, C., Li, Y., Lee, Y.J., 2023. Improved baselines with visual instruction tuning.

Liu, S., Ma, Y., Zhang, X., Wang, H., Ji, J., Sun, X., Ji, R., 2024a. Rotated multi-scale interaction network for referring remote sensing image segmentation, in: Proceedings of the IEEE/CVF Conference on Computer Vision and Pattern Recognition, pp. 26658–26668.

Liu, X., Lian, Z., 2024. RSUniVLM: A unified vision language model for remote sensing via granularity-oriented mixture of experts. arXiv preprint arXiv:2412.05679 .

Liu, Y., Li, H., Hu, C., Luo, S., Luo, Y., Chen, C.W., 2024b. Learning to aggregate multi-scale context for instance segmentation in remote sensing images. IEEE Transactions on Neural Networks and Learning Systems 36, 595–609.

Liu, Y., Peng, B., Zhong, Z., Yue, Z., Lu, F., Yu, B., Jia, J., 2025a. Seg-Zero: Reasoning-chain guided segmentation via cognitive reinforcement. arXiv preprint arXiv:2503.06520 .

Liu, Y., Qu, T., Zhong, Z., Peng, B., Liu, S., Yu, B., Jia, J., 2025b. VisionReasoner: Unified visual perception and reasoning via reinforcement learning. arXiv preprint arXiv:2505.12081 .

Loshchilov, I., Hutter, F., 2017. Decoupled weight decay regularization, in: International Conference on Learning Representations.

Lv, J., Shen, Q., Lv, M., Li, Y., Shi, L., Zhang, P., 2023. Deep learning-based semantic segmentation of remote sensing images: a review. *Frontiers in Ecology and Evolution* 11, 1201125.

Ma, X., Wu, Q., Zhao, X., Zhang, X., Pun, M.O., Huang, B., 2024. SAM-assisted remote sensing imagery semantic segmentation with object and boundary constraints. *IEEE Transactions on Geoscience and Remote Sensing* .

Osco, L.P., Wu, Q., De Lemos, E.L., Gonçalves, W.N., Ramos, A.P.M., Li, J., Junior, J.M., 2023. The Segment Anything Model (SAM) for remote sensing applications: From zero to one shot. *International Journal of Applied Earth Observation and Geoinformation* 124, 103540.

Ou, R., Hu, Y., Zhang, F., Chen, J., Liu, Y., 2025. GeoPix: A multimodal large language model for pixel-level image understanding in remote sensing. *IEEE Geoscience and Remote Sensing Magazine* , 2–16doi:[10.1109/MGRS.2025.3560293](https://doi.org/10.1109/MGRS.2025.3560293).

Pan, Y., Sun, R., Wang, Y., Zhang, T., Zhang, Y., 2024. Rethinking the implicit optimization paradigm with dual alignments for referring remote sensing image segmentation, in: Proceedings of the 32nd ACM International Conference on Multimedia, pp. 2031–2040.

Rasley, J., Rajbhandari, S., Ruwase, O., He, Y., 2020. DeepSpeed: System optimizations enable training deep learning models with over 100 billion parameters, in: Proceedings of the 26th ACM SIGKDD international conference on knowledge discovery & data mining, pp. 3505–3506.

Ravi, N., Gabeur, V., Hu, Y.T., Hu, R., Ryali, C., Ma, T., Khedr, H., Rädle, R., Rolland, C., Gustafson, L., et al., 2024. SAM 2: Segment anything in images and videos. arXiv preprint arXiv:2408.00714 .

Ren, S., Luzzi, F., Lahrichi, S., Kassaw, K., Collins, L.M., Bradbury, K., Malof, J.M., 2024a. Segment anything, from space?, in: Proceedings of the IEEE/CVF Winter Conference on Applications of Computer Vision, pp. 8355–8365.

Ren, Z., Huang, Z., Wei, Y., Zhao, Y., Fu, D., Feng, J., Jin, X., 2024b. PixelLM: Pixel reasoning with large multimodal model, in: Proceedings of the IEEE/CVF Conference on Computer Vision and Pattern Recognition, pp. 26374–26383.

Shao, Z., Wang, P., Zhu, Q., Xu, R., Song, J., Bi, X., Zhang, H., Zhang, M., Li, Y., Wu, Y., et al., 2024. DeepSeekMath: Pushing the limits of mathematical reasoning in open language models. arXiv preprint arXiv:2402.03300 .

Shen, H., Liu, P., Li, J., Fang, C., Ma, Y., Liao, J., Shen, Q., Zhang, Z., Zhao, K., Zhang, Q., et al., 2025. VLM-R1: A stable and generalizable R1-style large vision-language model. arXiv preprint arXiv:2504.07615 .

Su, H., Wei, S., Liu, S., Liang, J., Wang, C., Shi, J., Zhang, X., 2020. HQ-ISNet: High-quality instance segmentation for remote sensing imagery. *Remote Sensing* 12, 989.

Wang, D., Zhang, J., Du, B., Xu, M., Liu, L., Tao, D., Zhang, L., 2023. SAMRS: Scaling-up remote sensing segmentation dataset with segment anything model. *Advances in Neural Information Processing Systems* 36, 8815–8827.

Wang, J., Ke, L., 2024. LLM-Seg: Bridging image segmentation and large language model reasoning, in: Proceedings of the IEEE/CVF Conference on Computer Vision and Pattern Recognition, pp. 1765–1774.

Wang, J., Zheng, Z., Ma, A., Lu, X., Zhong, Y., 2021. LoveDA: A remote sensing land-cover dataset for domain adaptive semantic segmentation, in: Proceedings of the Neural Information Processing Systems Track on Datasets and Benchmarks.

Waqas Zamir, S., Arora, A., Gupta, A., Khan, S., Sun, G., Shahbaz Khan, F., Zhu, F., Shao, L., Xia, G.S., Bai, X., 2019. iSAID: A large-scale dataset for instance segmentation in aerial images, in: Proceedings of the IEEE/CVF conference on computer vision and pattern recognition workshops, pp. 28–37.

Xia, Z., Han, D., Han, Y., Pan, X., Song, S., Huang, G., 2024. GSVA: Generalized segmentation via multimodal large language models, in: Proceedings of the IEEE/CVF Conference on Computer Vision and Pattern Recognition (CVPR), pp. 3858–3869.

Xu, X., Feng, Z., Cao, C., Li, M., Wu, J., Wu, Z., Shang, Y., Ye, S., 2021. An improved swin transformer-based model for remote sensing object detection and instance segmentation. *Remote Sensing* 13, 4779.

Yang, S., Qu, T., Lai, X., Tian, Z., Peng, B., Liu, S., Jia, J., 2023. LISA++: An improved baseline for reasoning segmentation with large language model. arXiv preprint arXiv:2312.17240 .

Yao, L., Liu, F., Chen, D., Zhang, C., Wang, Y., Chen, Z., Xu, W., Di, S., Zheng, Y., 2025a. RemoteSAM: Towards segment anything for earth observation. arXiv preprint arXiv:2505.18022 .

Yao, L., Liu, F., Lu, H., Zhang, C., Min, R., Xu, S., Di, S., Peng, P., 2025b. RemoteReasoner: Towards unifying geospatial reasoning workflow. arXiv preprint arXiv:2507.19280 .

Yu, L., Poirson, P., Yang, S., Berg, A.C., Berg, T.L., 2016. Modeling context in referring expressions, in: European conference on computer vision, Springer. pp. 69–85.

Yuan, X., Shi, J., Gu, L., 2021. A review of deep learning methods for semantic segmentation of remote sensing imagery. *Expert Systems with Applications* 169, 114417.

Yuan, Z., Mou, L., Hua, Y., Zhu, X.X., 2024. RRSIS: Referring remote sensing image segmentation. *IEEE Transactions on Geoscience and Remote Sensing* 62, 1–12. doi:[10.1109/TGRS.2024.3369720](https://doi.org/10.1109/TGRS.2024.3369720).

Zhang, J., Zhou, Z., Mai, G., Hu, M., Guan, Z., Li, S., Mu, L., 2023. Text2seg: Remote sensing image semantic segmentation via text-guided visual foundation models. *arXiv preprint arXiv:2304.10597*.

Zhang, Z., Ma, Y., Zhang, E., Bai, X., 2025. PSALM: Pixelwise segmentation with large multi-modal model, in: European Conference on Computer Vision, Springer. pp. 74–91.

Zheng, Z., Zhong, Y., Zhang, L., Ermon, S., 2024. Segment any change. *Advances in Neural Information Processing Systems* 37, 81204–81224.

Zhou, Y., Lan, M., Li, X., Feng, L., Ke, Y., Jiang, X., Li, Q., Yang, X., Zhang, W., 2024. GeoGround: A unified large vision-language model for remote sensing visual grounding. *arXiv preprint arXiv:2411.11904*.

Zhu, J., Wang, W., Chen, Z., Liu, Z., Ye, S., Gu, L., Tian, H., Duan, Y., Su, W., Shao, J., et al., 2025. InternVL3: Exploring advanced training and test-time recipes for open-source multimodal models. *arXiv preprint arXiv:2504.10479*.

Appendix A. Instruction Template for the LVLM

To ensure that the LVLM produces consistent and correctly formatted outputs, we design a structured instruction template. As illustrated in Fig. [Appendix A.1](#), this template guides the LVLM by explicitly defining (i) the task to be performed, (ii) the requirement to generate a CoT reasoning process enclosed in `<think>` tags, and (iii) the JSON schema for the visual (geometric) prompts enclosed in `<answer>` tags. The generated geometric prompts are then passed to SAM for execution, making this template a critical component for the automated reasoning–execution pipeline.

Appendix B. Additional Qualitative Results

This appendix presents supplementary qualitative analyses to provide a broader and more nuanced view of the Think2Seg-RS framework. We first display additional results on the Earth-Reason dataset (Fig. [Appendix B.1](#)), illustrating the model’s robustness in handling complex and implicit queries. These

Instruction Template

```
Please find "{Question}", identify the target.
For each target instance, provide:
1. `bbox_2d`: A tight bounding box.
2. `positive_points`: Exactly two points, placed
inside the target.
Output your thinking process in <think> </think>
tags.
Output the final answer in <answer> </answer>
tags with the specified JSON format. If no
targets are found, output an empty list.
i.e.
<think> thinking process here </think>
<answer>```json[{"bbox_2d": [310,360,567,586],
"positive_points": [[434, 474], [450, 460]]},
{"bbox_2d": [10,200,100,320], "positive_points": [[50, 250], [90, 300]]}]```</answer>
```

Fig. [Appendix A.1](#): Structured instruction template for the LVLM. The template defines the task, the CoT reasoning format, and the required JSON schema for geometric prompts. The `{Question}` placeholder is dynamically replaced with the implicit, complex reasoning query for each input sample, ensuring that the LVLM generates consistent reasoning traces and well-formed prompts for downstream SAM execution.

examples highlight how the framework effectively bridges high-level semantic reasoning with the generation of precise geometric prompts.

Second, to provide a balanced evaluation, we analyze representative failure cases (Fig. [Appendix B.2](#)), which reveal limitations occurring at different stages of the decoupled pipeline. The first category involves high-level reasoning failures, where the LVLM misinterprets subtle query constraints, such as prioritizing the general concept of “regional development” over the specific function of “distributing electrical power”, leading it to misidentify a substation as a railway (first row). The second type, grounding ambiguity, arises even when reasoning is correct. In this case (second row), although the model correctly identifies a “factory,” it adopts an overly restrictive spatial scope, placing prompts only on the main building structures and thus missing the intended holistic area. A third error source is inaccurate prompt localization caused by strong visual distractors; for instance, the prominent shadow of a correctly identified “wind turbine” misleads the LVLM to place prompts on the shadow rather than the turbine itself (third row). The fourth row illustrates a semantic inconsistency between the region-level annotation of the dataset and the object-level perception inherent to the frozen SAM. Even with accurate reasoning and well-positioned prompts for a “major intersection,” the segmenter reasonably excludes transient objects such as vehicles, whereas the ground-truth mask defines the entire area as part of the intersection (fourth row).

Finally, Fig. [Appendix B.3](#) illustrates how the optimal prompt configuration varies with the geometric characteristics of the target. Although this adaptive selection mechanism is not yet implemented in the current framework, the examples provide an intuitive visualization of the direction discussed in our future work, where the LVLM could first infer the target’s structural type (e.g., regular, elongated, or irregular) and then dynamically

choose the most suitable combination of bounding boxes and points. This highlights the potential of extending Think2Seg-RS toward adaptive prompting strategies that generalize across diverse target geometries.

Together, these qualitative results complement the quantitative findings in the main paper, offering deeper insights into the behavior, strengths, and remaining challenges of Think2Seg-RS.



(a) Inputs

(b) Outputs

(c) GT Mask

Fig. Appendix B.1: Additional qualitative results of Think2Seg-RS on the EarthReason dataset. (a) Inputs, including the user query and corresponding remote sensing image. (b) Model outputs, comprising the LViM's reasoning text from the `<think>` stage, the generated geometric prompts (bounding box in red and positive points in green), and the resulting segmentation mask predicted by SAM2. (c) Ground-truth (GT) mask for reference.



Fig. Appendix B.2: Failure cases of Think2Seg-RS on the EarthReason dataset. (a) Inputs, including the user query and corresponding remote sensing image. (b) Model outputs, comprising the LVLM’s reasoning text from the <think> stage, the generated geometric prompts (bounding box in red and positive points in green), and the resulting segmentation mask predicted by SAM2. (c) Ground-truth (GT) mask for reference.

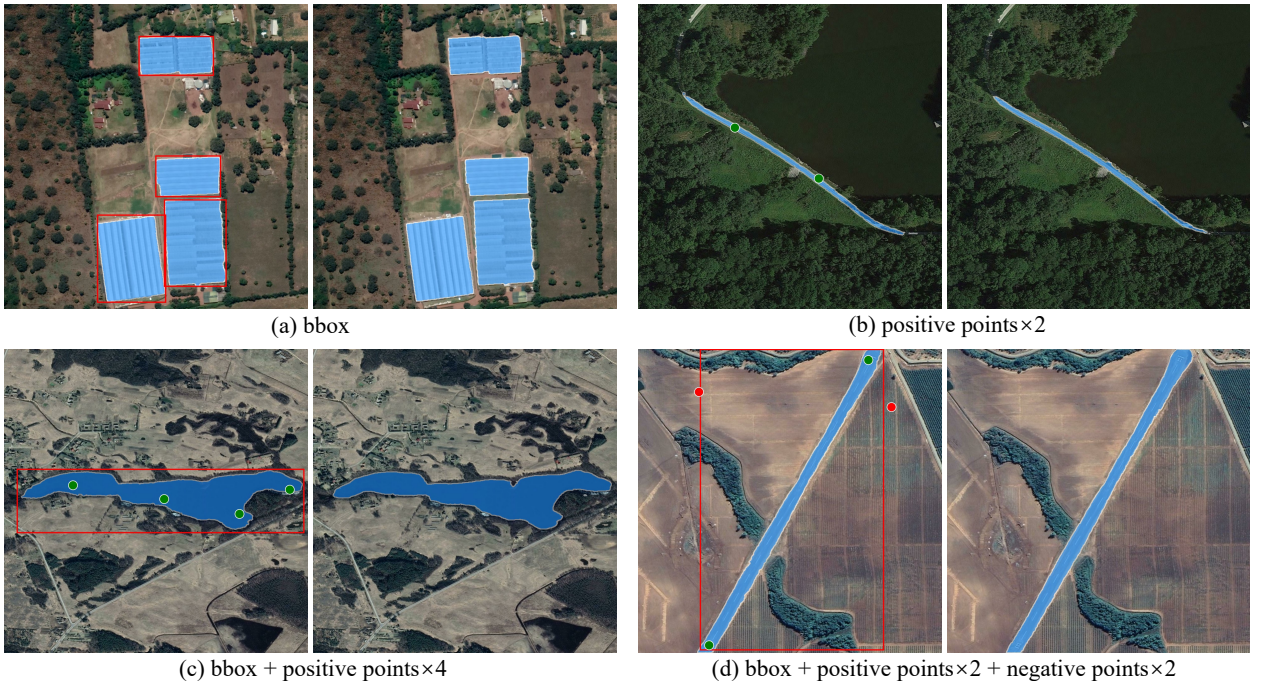


Fig. Appendix B.3: Examples of prompt combinations tailored to different target characteristics. Each pair displays the input image with generated prompts and the resulting segmentation mask (left, bounding boxes in red, positive points in green, negative points in red) and the ground truth mask (right). (a) For targets with regular, box-like geometries such as the greenhouses shown, a simple bounding box is effective and sufficient. (b) When segmenting thin, linear features like the narrow dam, two positive points placed along the object’s axis can define its trajectory precisely. (c) For objects with irregular and complex boundaries like the lake, a bounding box combined with multiple positive points is crucial for capturing the intricate details of the boundary. (d) In scenarios where a slender target occupies a small fraction of a bounding box, negative points become essential for explicitly excluding the large, visually similar background, thus preventing oversegmentation.